

Supplementary Information for:**Nanoparticle-mediated cellular response is size-dependent**

WEN JIANG^{1,2*}, BETTY Y. S. KIM^{1,2,3*}, JAMES T. RUTKA³ AND WARREN C. W. CHAN^{1,2†}

¹*Institute of Biomaterials and Biomedical Engineering, University of Toronto, 164 College Street, Toronto, Ontario M5S 3G9, CANADA*

²*Terrence Donnelly Centre for Cellular & Biomolecular Research, University of Toronto, 160 College Street, Toronto, Ontario M5S 3E1, CANADA*

³*Division of Neurosurgery, The Hospital for Sick Children, University of Toronto, 555 University Avenue, Toronto, Ontario M5G 1X8, CANADA*

**These authors contributed equally to this work.*

[†]email: warren.chan@utoronto.ca

ANTIBODY ADSORPTION

Proteins were adsorbed onto GNPs using the techniques developed by Geoghegan *et al*¹⁶. The optimum protein concentration required to stabilize a given solution of nanoparticles was determined by adding 10% NaCl to a series of nanoparticle solution with different protein added. The minimum protein concentration at which NaCl did not cause nanoparticle aggregation was determined to be the optimal protein concentration for conjugation.

The corresponding calculated protein amount was then added to 200 mL of the GNP solution at pH 8-9 while stirring for 1 min. A small volume of 10% Bovine Serum Albumen (BSA) (Sigma) solution was added to the mixture to bring its final concentration to 0.25% in order to prevent nanoparticle aggregation in solution. Following an additional 5 min. of stirring, the solution was transferred to a polycarbonate centrifuge tube (Nalgene Labware, Rochester, NY) and centrifuged at 15,000 g (4°C) for 1 h to remove unbound excess proteins. The pellet was resuspended in 0.01 M sodium phosphate buffer (pH 7.4) containing 0.25% BSA. Similar procedures were followed for silver nanoparticles (SNPs) of different sizes.

To determine the amount of proteins bound to the GNP surface, the solution was centrifuged at 15,000 g for 1 h and the supernatant protein concentration was measured using QuantiPro™ BCA Assay Kit (Sigma). The amount of protein bound to the surface of the GNP was calculated using the following formula: *Protein bound to gold nanoparticles = Total protein added – Protein in the supernatant solution.*

BINDING AVIDITY STUDY

SK-BR-3 cells were cultured in 96-well cell culture plates and grown to approximately 80% confluency. Cells were then fixed using a 1% paraformaldehyde fixative. Using varying concentrations of Herceptin modified GNPs, cells were incubated, fixed and blocked with BSA for 30 min. Once washed in PBS to remove the unbound GNPs, horseradish peroxidase labelled-IgG was added. Following a 2 h incubation, 2,2'-azino-bis(3-ethylbenzthiazoline-6-sulphonic acid (ABTS) was added. Absorbance measurements were performed using Sunrise Absorbance Reader (Tecan Group Ltd.). The dissociation constant was obtained by plotting the difference in the absorbance between Her-GNP coated cells and GNP coated cells as compared to the amount of Her-GNPs added to the cell culture. Non-specific binding was characterized using free GNPs and isotype-matched antibody modified GNPs.

GEL-ELECTROPHORESIS

Samples were mixed with 10% Ficoll solution (Sigma) and loaded onto 1% agarose gel (Sigma). Gel separation was performed using the electrophoresis unit running at 100 V (Fisher Scientific, UK). Protein levels were visualized by incubating the gels in Coomassie Brilliant Blue R-250 staining solution (Sigma). Gels were washed with a de-staining solution containing 70% methanol and 7% acetic acid and imaged using Kodak Imaging Station *In-Vivo* Imaging Systems (Kodak).

ELECTRON MICROSCOPY

GNPs were spread onto a carbon-coated copper grid. Once dried, Hitachi HD2000 STEM (Hitachi Corp, Japan) was used to image GNPs of various sizes. For cellular imaging, incubated cells were fixed for 3 h with Karnovsky's style fixative (4% paraformaldehyde, 2.5% glutaraldehyde in 0.1 M Sorensen's phosphate buffer, pH 7.2). Once washed with PBS for 15 min., cells were fixed with 1% osmium tetroxide for 1 h then dehydrated using a graded concentration series of ethanol. Epon resin infiltration using a graded series of ethanol was then polymerized in the plastic dishes at 40°C for 48 h. Various sections of the resin block were then cut using the Reichert Ultracut E microtome and transferred onto the 300 mesh copper TEM grids (Canemco-Marivac, Canada).

TUNEL ANALYSIS

Apoptosis was measured by incubating adherent cells for 72 h with free 40-nm GNPs, (Gold), free Herceptin (Her) and Herceptin modified GNPs of different sizes. All Herceptin concentrations were kept constant at 10 µg/mL. Using a cell scraper, cells were then harvested and centrifuged at 300 g for 5 min. to form a pellet. Cells were fixed with 1% paraformaldehyde and permeabilized using ice-cold ethanol. TUNEL assay was performed using the APO-BrdU assay kit (Phoenix Flow Systems, San Diego, CA). FITC positive cells were detected using flow cytometry. For cell cycle analysis, SK-BR-3 cells were trypsinized and fixed using ice-cold ethanol. To stain, cells were washed and resuspended in propidium iodide staining solution (3 µM PI, 100 mM Tris, pH 7.4, 150 mM NaCl, 1 mM CaCl₂, 0.5 mM MgCl₂, 0.1% NP-40 and 100 µg/mL RNase). Once incubated at room temperature for 15 min., cells were analyzed using flow cytometry. This procedure was repeated for free SNPs of different sizes, free Herceptin and Herceptin modified SNPs of different sizes.

WESTERN BLOT

Protein expression analysis was performed using previously published Western blot methods²⁵. Briefly, cells incubated in various conditions were washed 3 times using PBS. The concentration of antibody was kept constant throughout at 10 µg/mL. Cells were lysed using a NP40 lysis buffer (0.5% NP40, 150 mM NaCl, 20 mM Tris-HCl, 5 mM EGTA, 200 µM Na₃VO₄, 1 mM PMSF and 2 µg/mL leupeptin and aprotinin). Proteins were extracted by centrifugation and loaded onto a gel at a concentration of 50 µg per well. Total protein content was resolved using SDS-PAGE and transferred onto a nitrocellulose membrane. Specific proteins involved in ErbB2 signalling cascade such as phosphorylated-AKT (pAKT), phosphorylated-MAPK (pMAPK), Cyclin D1, p27, caspases 9 and caspase 3 were detected using primary antibodies (Cell Signal Technology, Beverly, MA) and horseradish peroxidase labelled goat anti-mouse IgG (Jackson Immuno Research, West Grove, PA). The labelled membranes were incubated in a ECL working solution before imaging with the VersaDoc Model 5000 BioRad Imaging System.

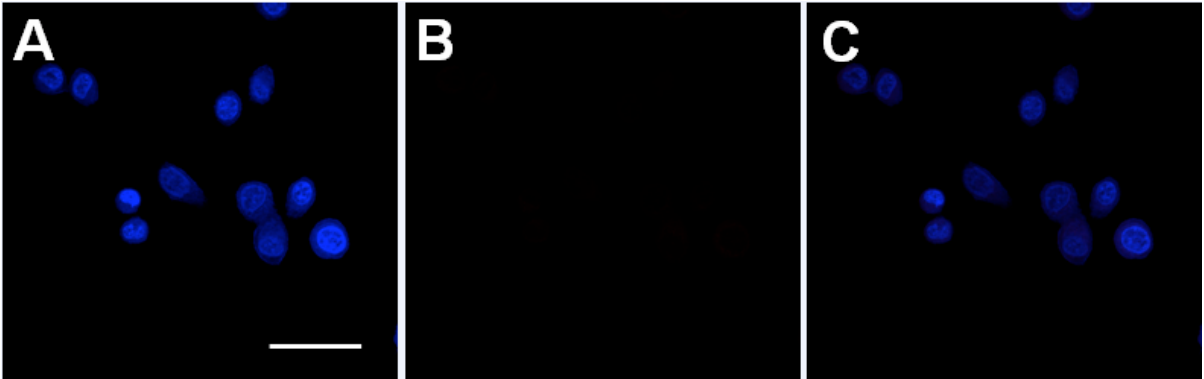


Figure S1: ErbB2 receptor fluorescence signal is specific. To eliminate the possibility of non-specific staining, we used an irrelevant antibody, anti-basic fibroblastic growth factor receptor (bFGFR-1) to label SK-BR-3 cells. Since these cells are known to have low bFGFR-1 membrane expression, minimal membrane labelling was observed. Cells were first labelled with anti-bFGFR-1 antibody and subsequently stained with (A) DAPI (blue channel). (B) Secondary mouse IgG conjugated to Alexa-633 dye molecules (red channel). (C) Overlay of (A) and (B). No significant fluorescent signal was detected, indicating minimal non-specific binding (scale bar = 10 μm).

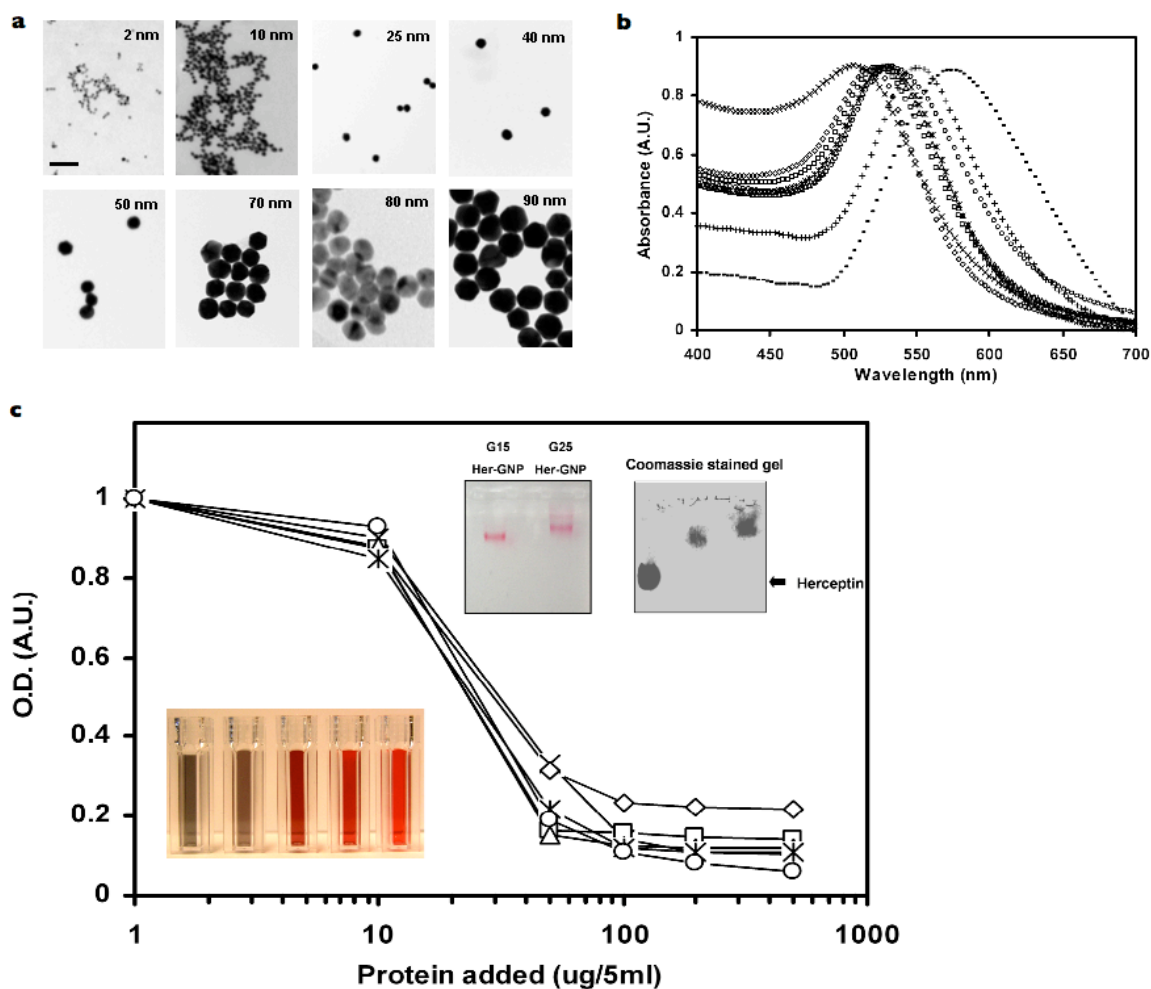


Figure S2: Systematic preparation and characterization of Herceptin adsorbed to gold nanoparticles (Her-GNPs) of different sizes. a, TEM images of GNPs (2-, 10-, 25-, 40-, 50-, 70-, 80- and 90-nm, respectively) (scale bar = 100 nm). b, UV-Vis absorbance measurements of GNPs with shift of the surface plasmon band peaks correlating with GNPs of different sizes. c, Her-GNP characterization. (Bottom inset) The determination of the optimal amount of Herceptin required for GNP stabilization. GNP aggregation was observed for protein concentrations < 10 $\mu\text{g}/\text{mL}$. (Top inset) Gel electrophoresis with and without Coomassie blue counter-staining demonstrated stable Herceptin adsorption with GNPs. The difference in the mobility of protein bands was attributed to the differences in the size of GNPs adsorbed to Herceptin (\times = 2 nm, \diamond = 10 nm, \square = 25 nm, \triangle = 40 nm, $*$ = 50 nm, \circ = 70 nm, $+$ = 80 nm and $-$ = 90 nm).

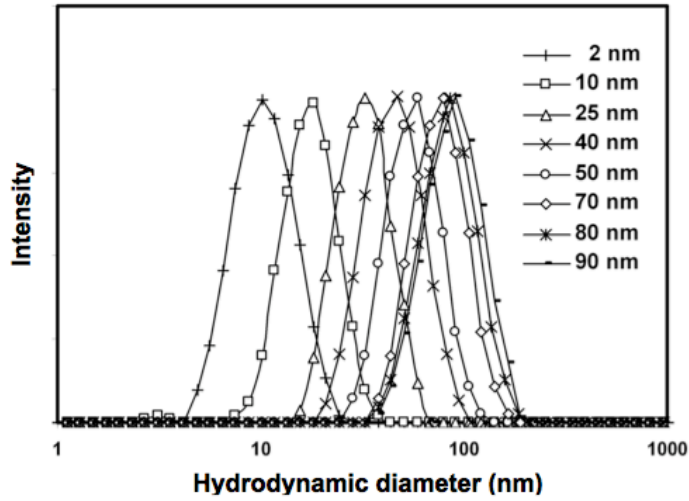


Figure S3a: Hydrodynamic diameter measurements of GNPs of different sizes using dynamic light scattering.

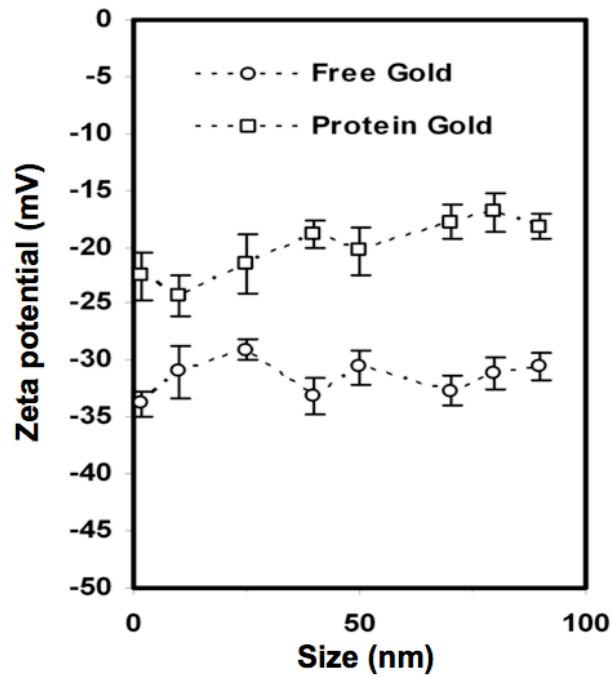


Figure S3b: Zeta potential measurements of GNPs before and after Herceptin adsorption. At physiological pH, the addition of Herceptin to the GNPs increased the average zeta potential value.

Gold Nanoparticle	Unmodified			Modified with Herceptin	
	Hydrodynamic Diameter (nm)	Zeta Potential (mV)	Aspect Ratio	Hydrodynamic Diameter (nm)	Zeta Potential (mV)
2 nm	7.9 ± 0.8	-33.8 ± 1.1	1.042 ± 0.012	13.7 ± 0.9	-22.5 ± 2.1
10 nm	17.8 ± 1.1	-31 ± 2.3	1.067 ± 0.019	25.6 ± 1.2	-24.3 ± 1.8
25 nm	33.6 ± 1.5	-29.1 ± 0.9	1.1 ± 0.033	44.5 ± 1.7	-21.5 ± 2.6
40 nm	47.8 ± 2.3	-33.2 ± 1.6	1.14 ± 0.049	66.5 ± 2.7	-18.8 ± 1.2
50 nm	57.5 ± 2.7	-30.6 ± 1.5	1.16 ± 0.057	79.2 ± 3.4	-20.3 ± 2.1
70 nm	78.1 ± 3	-32.7 ± 1.3	1.11 ± 0.041	98.5 ± 4.1	-17.8 ± 1.5
80 nm	85.9 ± 3.5	-31.1 ± 1.4	1.18 ± 0.062	108.3 ± 4.8	-16.9 ± 1.7
90 nm	96.8 ± 4.1	-30.5 ± 1.2	1.22 ± 0.067	119.3 ± 4.6	-18.2 ± 1.1

n = 50 for aspect ratio measurements

Table S1: Characterization of GNPs of different sizes before and after Herceptin adsorption. Key parameters including zeta potential and aspect ratio (the long axis divide by the short axis of GNPs) remained relatively constant for all GNP sizes. The modification of GNPs with Herceptin slightly increased the zeta potential at physiological pH. For free GNPs, the hydrodynamic diameter increased linearly with respect to the increase in nanoparticle size. Following Herceptin adsorption, the hydrodynamic diameter increased non-linearly for GNPs within 2- to 50- nm size-range, indicating possible protein posture rearrangement on GNP surfaces for optimal protein loading. Aspect ratio measurements were performed by measuring the ratio between the long-axis and short axis of the nanoparticles from representative TEM images of the sample.

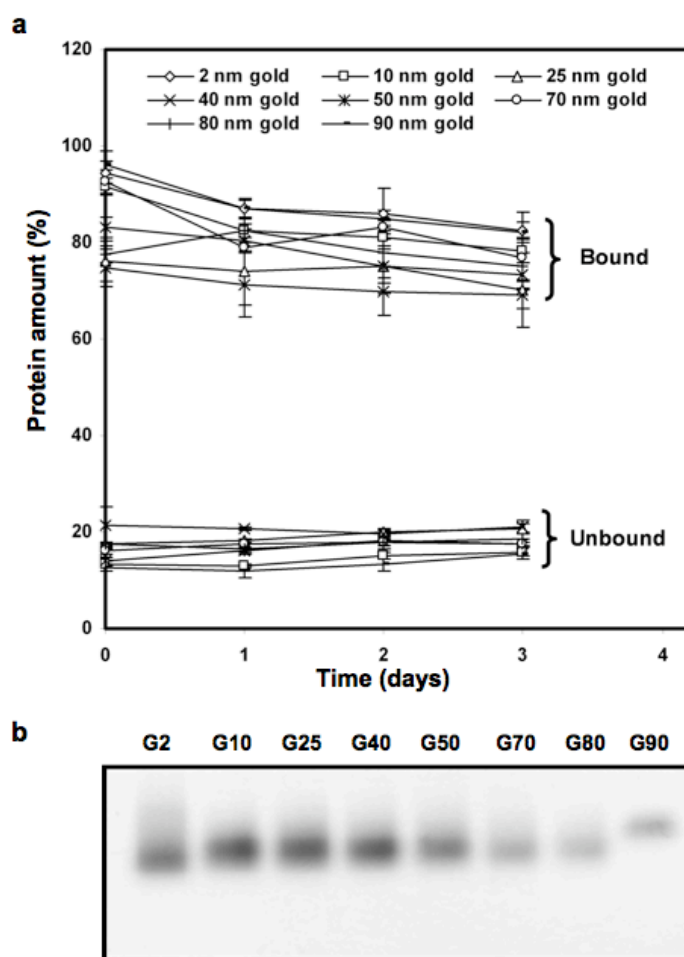


Figure S4: Desorption kinetics characterization of Herceptin from the GNP surface in phosphate buffer solution (pH 7.4). a, Following three days of incubation, the amount of Herceptin adsorbed onto the GNP surface was slightly decreased (<10%). Since the unbound Herceptin in solution was measured to increase over time, the loss of bound Herceptin was contributed to their desorption from the particle surface. Overall, both bound and unbound Herceptin constituted approximately 100% of the total Herceptin added, indicating negligible protein loss during experimental procedures. b, To qualitatively confirm the presence of Herceptin on the surface of GNPs, detection of Herceptin on GNPs were resolved using gel electrophoresis with Coomassie blue protein counter-staining. The difference in the mobility of protein bands was attributed to the differences in the size of GNPs. The gel image provides a qualitative indication of the antibody bound to the GNPs following three days of incubation. All lanes were loaded with equal volumes of Her-GNP solutions.

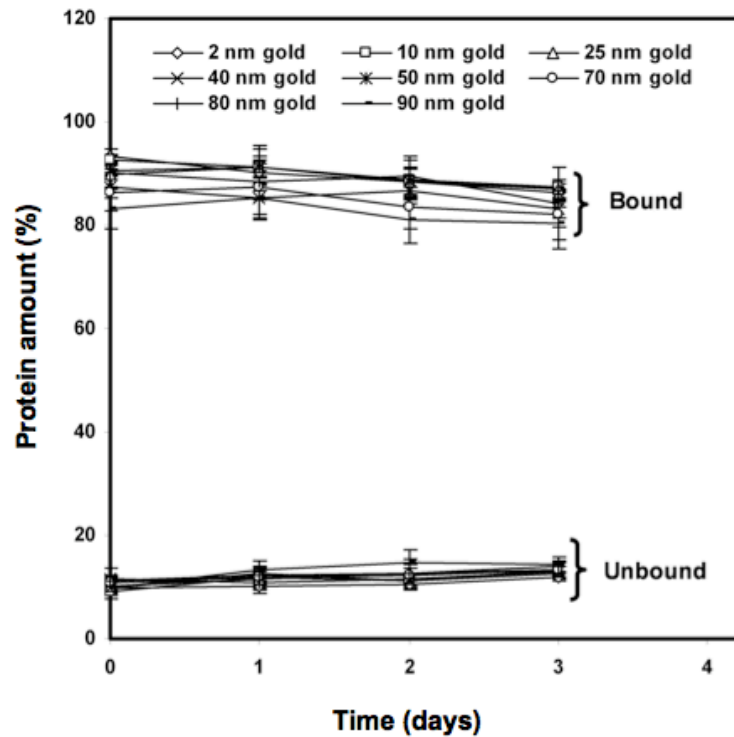


Figure S5: Desorption kinetics characterization of Herceptin from the GNP surface in cell culture media. To elucidate whether cell culture media affected the desorption of Herceptin from the GNP surface, the amount of Herceptin bound to either GNPs or in solution was measured over a period of three days. Since cell culture media often contain proteins, we used horse radish peroxidase (HRP) conjugated IgG to specifically detect the presence of Herceptin. Interestingly, Herceptin desorption from the GNP surface was much less in cell culture media compared to the phosphate buffer solution. The presence of proteins in media (such as fetal bovine serum) provided further stabilization of the Herceptin-GNP complex, which reduced Herceptin desorption from the GNP surface.

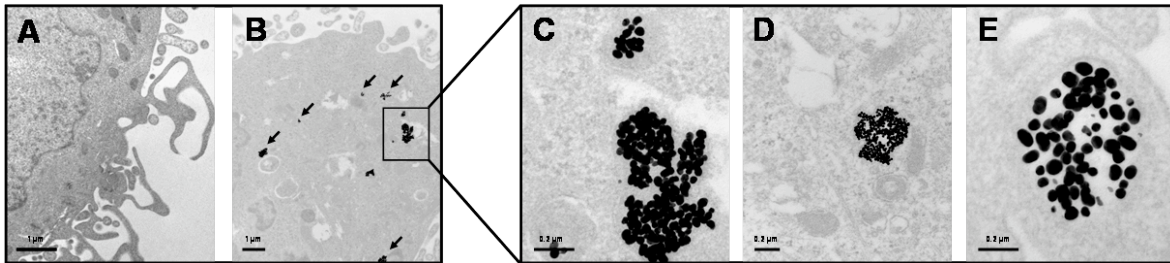


Figure S6: TEM images of cellular uptake of Her-GNPs and free GNPs. (A) Cells incubated with unmodified 40-nm GNPs exhibited minimum or no uptake of nanoparticles after 3 h incubation. (B) The intracellular uptake of nanoparticles was significantly enhanced with G40 Her-GNP treatment at the same nanoparticle concentration. The minimal free nanoparticle uptake was attributed to the low concentration of nanoparticles utilized (G40 ~ 100 fM) as compared to previously published studies (>10 pM)¹⁷. Despite the reduction in GNP concentrations, the process of cellular uptake was highly efficient for Herceptin adsorbed nanoparticles. A significant amount of Her-GNPs accumulated within vesicle-like cytoplasmic structures. (C-E) Multiple enlarged views of representative samples with enhanced Her-GNP uptake.

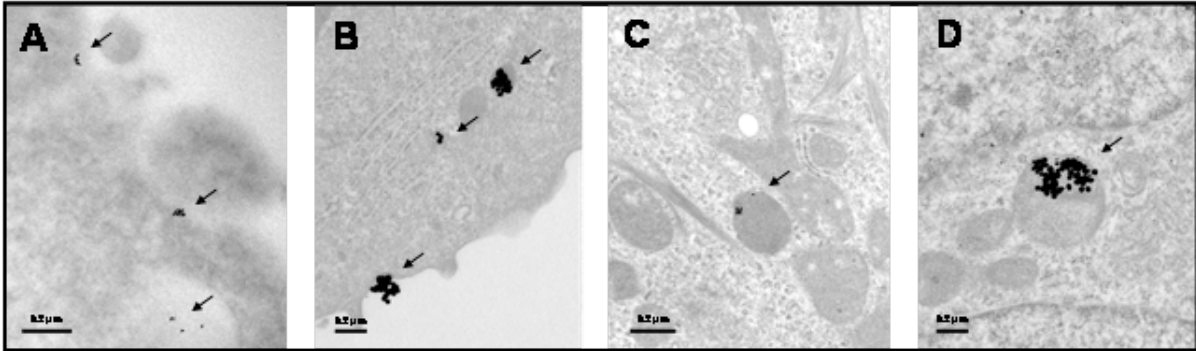


Figure S7: TEM images of cellular uptake of Her-GNPs of different sizes. (A) G2 Her-GNPs exhibited lower uptake efficiency as compared to (B), G40 Her-GNPs. (A,C) Limited sequestration of nanoparticles within cytoplasmic vesicles was observed following 3 h incubation with G2 Her-GNPs treatment. (B,D) In contrast, G40 Her-GNP treated cells exhibited a much higher intracellular uptake of nanoparticles. A significant number of G40 Her-GNPs was found within cytoplasmic vesicles.

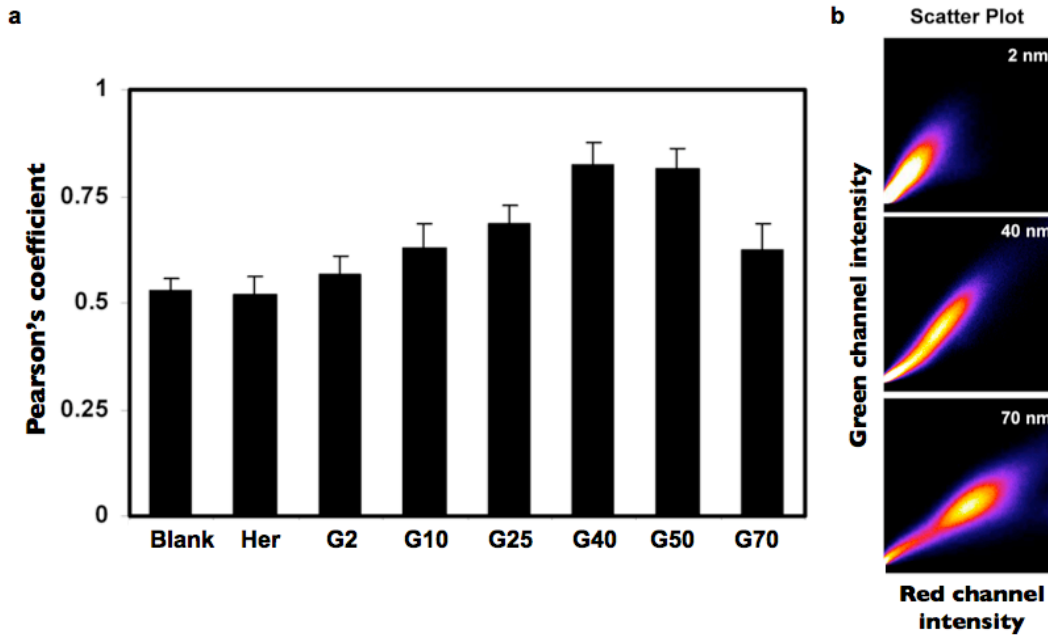


Figure S8: Quantitative analysis of ErbB2 co-localization with transferrin receptors following Her-GNP treatment. a, Pearson's correlation coefficient was obtained by measuring the scatter plot of red and green channel fluorescence intensity corresponding to the ErbB2 and transferrin receptors, respectively. As demonstrated by the greatest Pearson's correlation coefficient, co-localization was best observed in cells treated with G40 Her-GNPs as compared to other sizes of Her-GNPs. b, Scatter plot showing the correlation between red (ErbB2 receptor) and green (transferrin receptor) fluorescence channels. G40 Her-GNP treated cells demonstrated higher correlation between the two channels as compared to G2 and G70 Her-GNP treated cells. Image analysis was performed using ImageJ software.

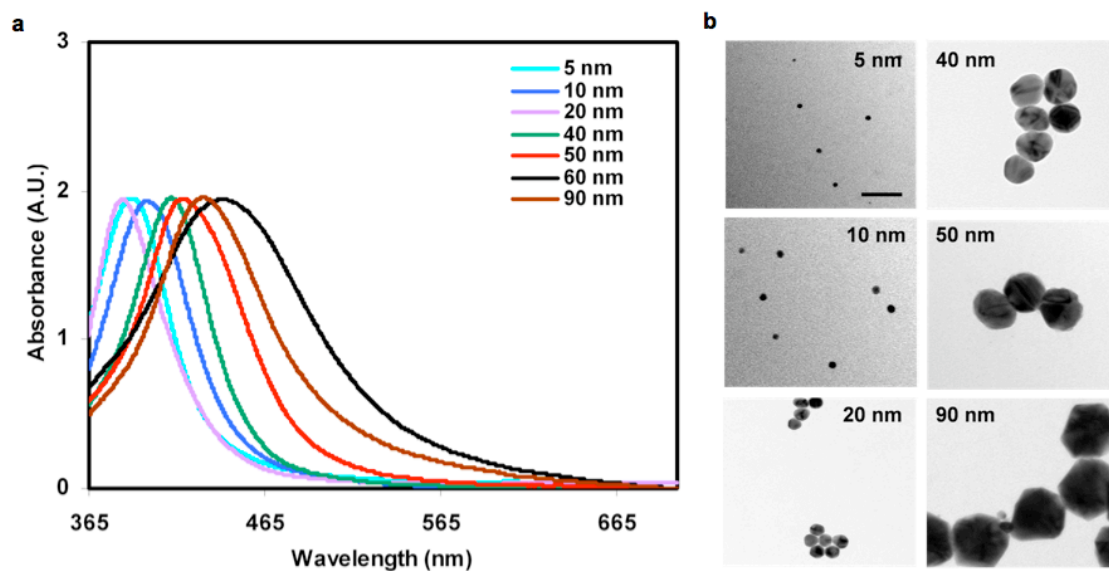


Figure S9: Systematic preparation and characterization of Herceptin modified silver nanoparticles (Her-SNPs) of different sizes. a, UV-Vis absorbance measurements of SNPs demonstrated the size-dependent shift of the surface plasmon band peaks. b, TEM images of SNPs (5-, 10-, 20-, 40-, 50- and 90-nm) (scale bar = 50 nm).

Silver Nanoparticle	Unmodified			Modified with Herceptin	
	Hydrodynamic diameter (nm)	Zeta Potential (mV)	Aspect Ratio	Hydrodynamic diameter (nm)	Zeta Potential (mV)
5 nm	10.3 ± 0.5	-20.7 ± 0.6	1.052 ± 0.026	15.5 ± 0.7	-16.6 ± 1.4
10 nm	16.7 ± 0.8	-21.2 ± 1.1	1.063 ± 0.021	23.4 ± 0.8	-15.4 ± 1.6
20 nm	25.8 ± 1.1	-22.2 ± 1.3	1.071 ± 0.025	34.9 ± 0.9	-15.7 ± 1.5
40 nm	46.6 ± 1.2	-20.9 ± 1.4	1.065 ± 0.028	56.7 ± 1.1	-16.3 ± 1.3
50 nm	55.7 ± 1.4	-20.4 ± 1.3	1.067 ± 0.029	68.5 ± 1.2	-16.8 ± 1.4
60 nm	68.5 ± 1.4	-22.4 ± 1.7	1.073 ± 0.027	81.6 ± 1.3	-16.6 ± 1.7
90 nm	97.3 ± 1.5	-20.2 ± 1.3	1.077 ± 0.031	114.7 ± 1.5	-17.1 ± 1.8

n = 50 for aspect ratio measurements

Table S2: Characterization of SNPs of different sizes before and after Herceptin adsorption. Key parameters including zeta potential and aspect ratio remained constant for all SNP sizes. SNP modification with Herceptin increased the zeta potential at physiological pH.

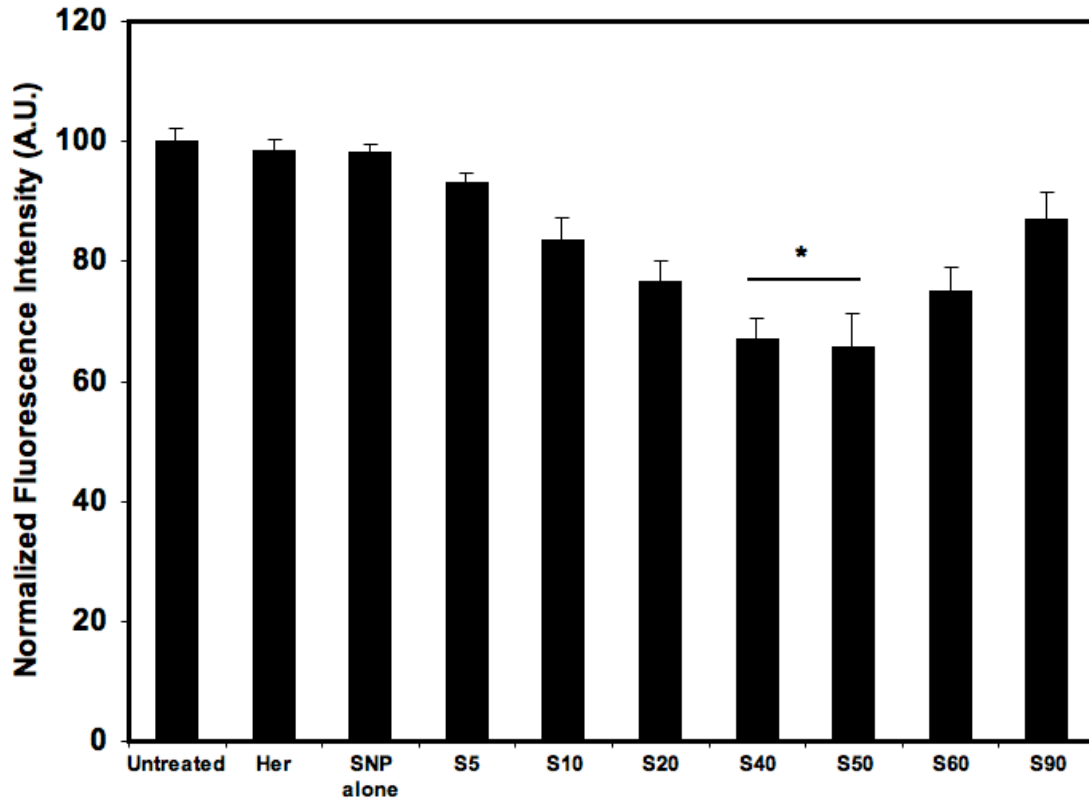


Figure S10: Down-regulation of membrane ErbB2 expression induced by Her-SNPs of different sizes. Flow cytometry analysis of surface ErbB2 expression using fluorescence intensity as an indicator of membrane receptor expression level. All fluorescence intensity was normalized using untreated cells (Untreated) as 100% expression level. Cells were treated with free Herceptin (Her), unmodified 40-nm SNPs (SNP alone) and Herceptin modified SNPs of various sizes (5-, 10-, 20-, 40-, 50-, 60- and 90-nm). Similar to the trend observed using Her-GNPs, the most significant reduction in ErbB2 membrane expression level was observed with S40 and S50 Her-GNP treatment (* denote statistical significance for S40/S50 compared to other sized Her-GNP, $p < 0.1$ ANOVA). Error bars, \pm s.d. ($n = 3$).

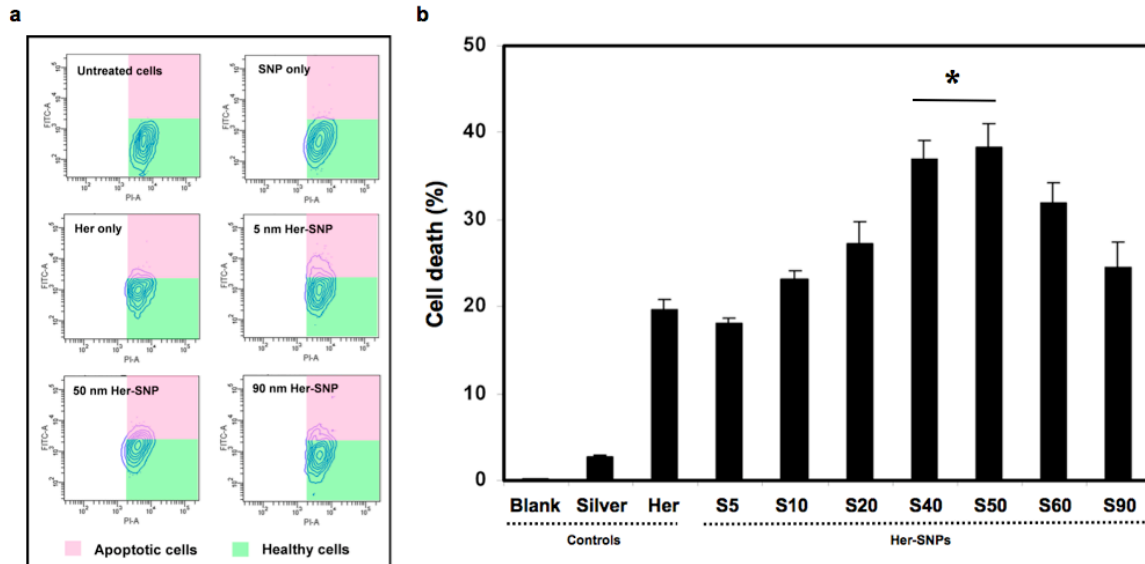


Figure S11: Modulating cellular function using Herceptin modified SNPs of different sizes. Apoptotic cells were measured following treatment with unmodified 40-nm SNPs (Silver), free Herceptin (Her) and Herceptin modified with SNPs of different sizes (5-, 10-, 20-, 40-, 50-, 60- and 90- nm). a, Flow cytometry was used to measure the percentage of healthy and apoptotic cells in a given population under different treatment conditions. b, The percentage of cells that undergo apoptosis was more significant for cells treated with S40 and S50 Her-SNPs as compared to Herceptin alone, or with other sizes of Her-SNPs (* denotes statistical significance for S40/S50 compared to other sized Her-GNP, $p < 0.05$, ANOVA). Error bars, \pm s.d. ($n = 3$).

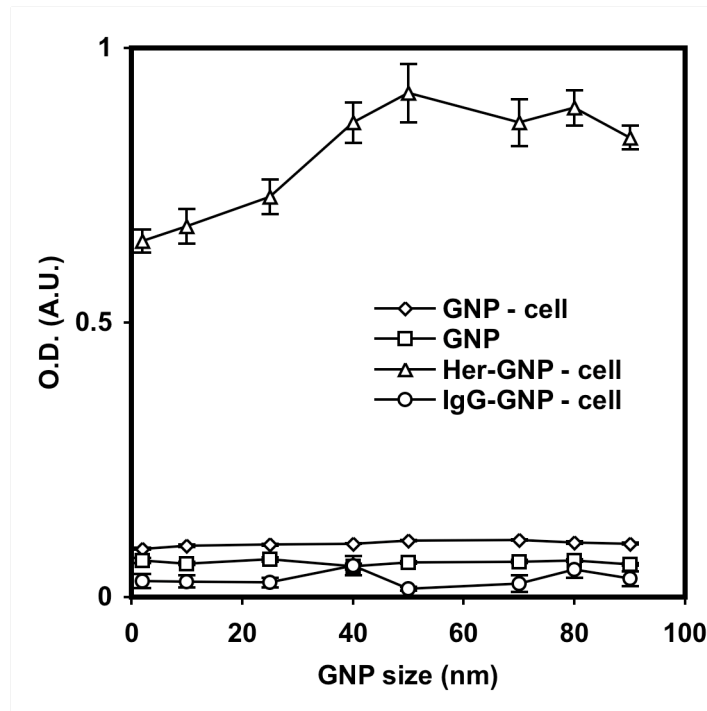


Figure S12: GNP binding study. Unmodified GNPs of different sizes were incubated in microwell plates coated with either SK-BR-3 cells (GNP-cell) or with BSA (GNP). For both conditions, negligible non-specific binding was observed, as the measured absorbance values were insignificant when compared to Her-GNPs of corresponding sizes. In addition, the modification of GNPs with irrelevant goat anti-mouse IgG antibody (IgG-GNP) resulted in an even lower degree of binding when incubated with cells possibly due to the fact that the monoclonal antibody was purified to reduce non-specific binding. These results suggest that the majority of interactions observed in Her-GNPs occurred through specific binding between Her-GNPs and cell surface receptors. These interactions were found to be dependent on size (shown in Figure 1c). The non-specific interactions and inherent optical characteristics of cells, buffer and microwell plates were considered for the binding measurements.